

Effect of pore pressure distribution on dynamic deformation moduli of soft clays

Rigoberto Rivera, Carmelino Zea, Enrique Elizalde

Division of Civil Engineering and Geomatics - Faculty of Engineering, National Autonomous University of Mexico, Mexico City, Mexico, riverac@unam.mx, zeaconcar@hotmail.com, eelizalder@yahoo.com.mx

Oswaldo Flores, Alexandra Ossa, Enrique Gómez, Mary Morante

Institute of Engineering, National Autonomous University of Mexico, Mexico City, Mexico, OFloresC@iingen.unam.mx, AOssaL@iingen.unam.mx, EGomezR@iingen.unam.mx, mmoranteg@iingen.unam.mx

ABSTRACT: The dynamic deformations moduli and the material damping were measured in specimens of unaltered clays from Mexico City, in undrained conditions, using automated cyclic triaxial equipment that allowed controlling the application of cyclic vertical deviator stresses (controlled stress or strain) and measuring the pore pressures generated during the test at the base and head of the specimen. The tests were in stress-controlled mode, using frequencies of 0.5 Hz and 1.0 Hz as this is a representative value for most earthquakes in Mexico City. Once the clay specimens were consolidated to the equivalent effective in-situ stress state (σ'_{co}), they were subjected to a normal cyclic deviator stress $\pm\Delta p_z$ applying a load cycles number $N = 20$, for each increment, until failure was reached. During the application of the cyclic deviatoric stresses, the linear strains were measured for both compression and stress relief, these values together with the Poisson's ratio and based on Zeevaert's analytical model, they allowed the corresponding dynamic deformation moduli to be calculated. The results obtained showed the influence of pore pressure distribution in the determination of the dynamic deformation moduli for soils with very low permeability, such as the soft clays of the Mexico City.

KEYWORDS: Cyclic behaviour, Dynamic parameters, Zeevaert's model, Cyclic pore pressure, Soft clays.

1 INTRODUCTION

The pore pressure generated during a monotonic, undrained triaxial test depends mainly on the mechanical properties of the tested soil and the imposed strain rate. Since pore pressure is generally measured at the base of the specimen, in high-permeability soils it can be assumed that this pressure is substantially uniform along the specimen; however, in highly plastic soft clays with very low permeability, this condition is not met (Josseaume H, 1971), (Kimura and Saitoh, 1983), (Rojas, Romo and Hiriart, 1990). These researchers point out that the strain rate adopted in the test must be compatible with the response time of the pore pressure measurement device used and with the corresponding equalization time throughout the specimen. Regarding the measurement device, the delay in response is due to the fact that the transducer membrane must deform to register an increase in pore pressure, and for this to occur, there must be a flow of water from the specimen to the transducer. However, due to the low permeability of plastic clayey soils, water flow is not immediate, which explains the delay in response.

On the other hand, it is recognized that during the test the state of deformations in the specimen is not uniform, due to the displacement restrictions imposed by the boundary conditions at both the head and base of the specimen. Even when lubricated surfaces are used to minimize this effect, the shear stresses generated during the test are higher in the central part of the specimen than at the ends. Therefore, it is concluded that pore pressures are not uniform, being higher at the base of the specimen and lower at the center. According to (Josseaume H, 1971), this phenomenon will be much more important in preconsolidated soft clays with very low permeability, tested at very high strain rates (>0.02 mm/min), and to a lesser extent in normally consolidated soft clays tested at the same strain rate. When the latter was 10 times lower (0.002 mm/min), the differences between pore pressures measured at the center and base of the specimen were much smaller and of the same order of magnitude for strains near failure.

In the case of undrained cyclic triaxial tests performed on saturated low-permeability clays, the pore pressures generated during the test are still measured at the base of the specimen ((Yasuhara, Yamanouchi and Hirao, 1982), (Hyodo,

Yamamoto and Sugiyama, 1994), (Soralump and Prasomsri, 2016), (Huang et al., 2023)), with the uncertainties already mentioned for monotonic triaxial tests regarding the response time of the measurement device and the equalization time of pore pressure along the soil specimen. In the case of the very soft lacustrine clays of Mexico City (CDMX), this has been no exception ((Mendoza and Hernández, 1994), (Ovando et al., 2021), (Rivera et al., 2024)); pore pressure measurement during cyclic triaxial tests has been at the base of the specimen, with test frequencies between 0.25 and 1.0 Hz.

(Zeevaert, 1988) had already pointed out this problem of delay in the response of the measurement equipment and the equalization time of pore pressure for the case of the soft clays of Mexico City, and its effect on the determination of the corresponding dynamic parameters. Given the uncertainty of the real value of pore pressure generated during the test, this researcher proposes an iterative methodology to estimate this pressure, in compression or tension, for a given strain level, based on the applied cyclic deviator stress, the ratio of deformation moduli and their response, as well as the tension moduli and their response. The first results obtained in soft clays of Mexico City, subjected to undrained cyclic triaxial tests under stress control, with a frequency of cyclic deviator stress application of 0.5 Hz, showed that the pore pressures measured at the base of the specimen and those determined with Zeevaert's methodology (Zeevaert, 1988) are of the same order of magnitude and do not exceed the value of 0.20 for the pore pressure/effective consolidation vertical stress ratio (Rivera et al., 2024).

Given this scenario, it is necessary to know the true distribution of pore pressure along the specimen to rationally interpret cyclic triaxial tests in highly plastic low-permeability soft clays. For this reason, in this research, the pore pressure generated during the application of cyclic deviator stress will be measured at the head and base of the specimen. This will allow making a comparison between the measured values and those calculated with Zeevaert's model and deriving from it the deformation moduli most representative of the cyclic behavior of the soft clays of Mexico City.

2 DESCRIPTION OF THE CYCLIC TRIAXIAL CHAMBER USED IN THE TESTS

The cyclic triaxial equipment (Figure 1) consists of an acrylic chamber [A] that houses the soil specimen protected by a latex membrane. The pressures with which the specimen is confined (confinement pressure) and that applied to the inside (back pressure) are made using the sensors [B], which in our case have a measurement range of 0 to 700 kPa, approximately.

The volume change [C] is recorded with a sensor formed by an acrylic cylinder that holds the water entering or leaving the specimen and generates a displacement of a piston, which, from this signal and the area of the cylinder, quantifies the volume of water entering or leaving the specimen.

It also has an axial displacement sensor [D] with a 50 mm total stroke, located at the top of the equipment, and a hydrostatically compensated load cell [E] with a 1.0 kN capacity, located at the base of the chamber, in direct contact with the soil specimen. These two sensors, in addition to recording the displacement and axial load experienced by the specimen, allow test control with monotonic or cyclic excitation under displacement or stress control.

The excitation system is pneumatic, with the support of a servo-valve [F] and a piston [G] located on the equipment's loading frame [H]. The servo-pneumatic control system synchronizes the flow of compressed air passing through the servo-valve to the piston to apply a monotonic or cyclic displacement pattern, operating the equipment under displacement or load control, with the support of the corresponding sensors.

All the sensors and the servo-pneumatic system must be calibrated and experimentally verified to obtain the calibration constants and the accuracy of each sensor.

The excess pore pressures at the base [I] and at head [J] of specimen recorded during the application the deviator cyclic stress (Figure 2) are made using the pore pressure sensors, having a measurement range of 0 to 700 kPa, approximately. To ensure that the pore pressures measured at the top and base of the specimen were not influenced by the flexibility of the measurement system, the connecting hoses of the two pressure transducers were made as rigid and as short as possible, thereby minimizing unwanted volume changes during undrained tests.

The signals received by the equipment, including axial deformation, load, pressures, and volumetric change, are transmitted to the computer via an analog-to-digital converter and processed using software developed in *Labview*.

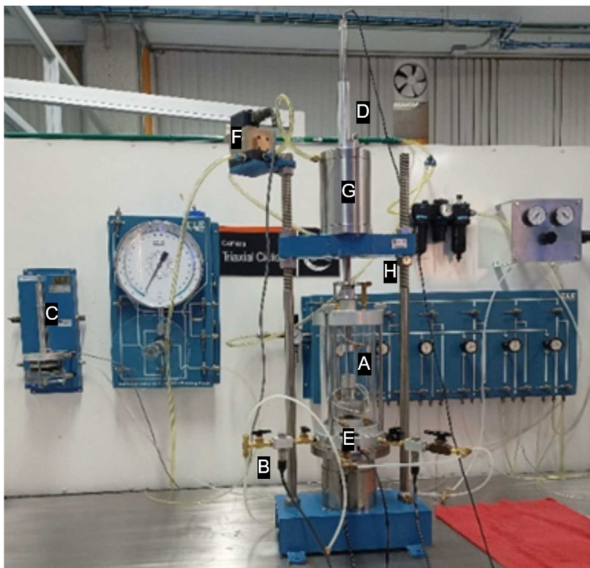


Figure 1. Cyclic triaxial apparatus components



Figure 2. Pore pressure transducer at base and head of the specimen

3 DYNAMIC UNIT DEFORMATION MODULI

Different procedures have been developed to measure the dynamic properties of soils, considering the range of deformations that an earthquake can generate in the subsoil.

Currently, few equipment can cover the entire range of deformations required in dynamic problems, apart from the Hollow Cylinder Torsional Shear Apparatus (Gasparre et al., 2007). Therefore, from a practical engineering point of view, it is common to combine available equipment to cover the range of deformations of interest.

In the undrained cyclic triaxial tests performed in this research, the pore pressures generated by the application of cyclic deviator stress were measured at the base and head of the specimen, this allowed compare the calculated values with the theoretical estimation of pore pressure using Zeevaert's model (1988) and established the representative dynamic deformations moduli of the material tested.

Zeevaert's Model (Zeevaert, 1988) allows analytically estimating the increase in pore pressure generated during the application of a cyclic deviator stress $\pm \Delta p_z$. For this, it is necessary to know the vertical strains in both compression and tension, Poisson's ratio (ν), the degree of saturation (S_w), porosity (n), and the ratios of dynamic unit deformation moduli: compression-response (β_{cz}) and tension-response (β_{ez}), called soil response factors. It is assumed that during the short time of cyclic load application there is no dissipation of pore pressure.

For the cyclic vertical stress in compression, $+\Delta p_z$, the pore pressure, $\Delta \omega_c$, can be calculated as:

$$\Delta \omega_c = -\frac{b}{2a} + \sqrt{\left(\frac{b}{2a}\right)^2 + \frac{c}{a}} \quad (1)$$

$$a = 1 - \frac{n(1 - S_w)(1 - 2\nu\beta_{cz})}{(1 + 2\beta_{cz})(1 - 2\nu)\Delta \epsilon_{zc}} \quad (2)$$

$$b = p_a + \left\{ \frac{n(1 - S_w)}{(1 - 2\nu)\Delta \epsilon_{zc}} - 1 \right\} \frac{\Delta p_{zc}}{1 + 2\beta_{cz}} \quad (3)$$

$$c = \frac{p_a}{(1 + 2\beta_{cz})} \Delta p_{zc} \quad (4)$$

Where p_a is the atmospheric pressure and $\Delta \varepsilon_{zc}$ is the vertical unit strain (z-axis) in compression.

For the cyclic vertical stress in tension, $-\Delta p_z$, the pore pressure, $\Delta \omega_t$, can be calculated as:

$$\Delta \omega_t = \frac{\bar{b}}{2\bar{a}} - \sqrt{\left(\frac{\bar{b}}{2\bar{a}}\right)^2 + \frac{\bar{c}}{\bar{a}}} \quad (5)$$

$$\bar{a} = 1 + \frac{n(1 - S_w)(1 - 2\nu\beta_{ez})}{(1 + 2\beta_{ez})(1 - 2\nu)\Delta \varepsilon_{zt}} \quad (6)$$

$$\bar{b} = \left(1 + \frac{n(1 - S_w)}{(1 - 2\nu)\Delta \varepsilon_{zt}}\right) \frac{\Delta p_{zt}}{1 + 2\beta_{ez}} + p_a \quad (7)$$

$$\bar{c} = \frac{-1}{(1 + 2\beta_{ez})} p_a \Delta p_{zt} \quad (8)$$

Where $\Delta \varepsilon_{zt}$ is the vertical linear strain (z-axis) in tension.

Knowing the theoretical value of the pore pressure increment $\Delta \omega_c$ in compression and assuming an initial value of the response factor β_{cz} , it is possible to determine the unit deformation modulus in compression (M_{cz}) as:

$$M_{cz} = \frac{\Delta \varepsilon_{zc}}{\Delta p_{zc} - (1 - 2\nu\beta_{cz})\Delta \omega_c} \quad (9)$$

Meanwhile, the unit deformation modulus for the response in compression is calculated as:

$$M_{ex} = \frac{\Delta \varepsilon_{zcr}}{\Delta p_{zc} - (1 - 2\nu)\Delta \omega_c} \quad (10)$$

Thus, the response factor β_{cz} is calculated as:

$$\beta_{cz} = M_{ex}/M_{cz} \quad (11)$$

With the calculated value of the response factor β_{cz} , the calculation process is repeated iteratively, Equations (1) to (4), until Equations (9) and (10) are satisfied, thus obtaining the real response factor in compression.

For the cyclic vertical stress in tension, $-\Delta p_z$, the pore pressure, $\Delta \omega_t$, can be calculated following a similar iterative process to that described for cyclic vertical stress in compression, but now using the following equations:

$$M_{ez} = \frac{\Delta \varepsilon_{zt}}{\Delta p_{zt} - (1 - 2\nu\beta_{ez})\Delta \omega_t} \quad (12)$$

$$M_{cx} = \frac{\Delta \varepsilon_{ztr}}{\Delta p_{zt} - (1 - 2\nu)\Delta \omega_t} \quad (13)$$

$$\beta_{ez} = M_{cx}/M_{ez} \quad (14)$$

Figure 3 shows schematically the procedure to obtain the parameters of Zeevaert's model (Zeevaert, 1988) through a stress-controlled cyclic triaxial test for a soil specimen tested normal to stratification. Finally, the parameters of the model are: M_{cz} , M_{ez} , M_{cx} , M_{ex} , $\Delta \omega_c$, and $\Delta \omega_t$.

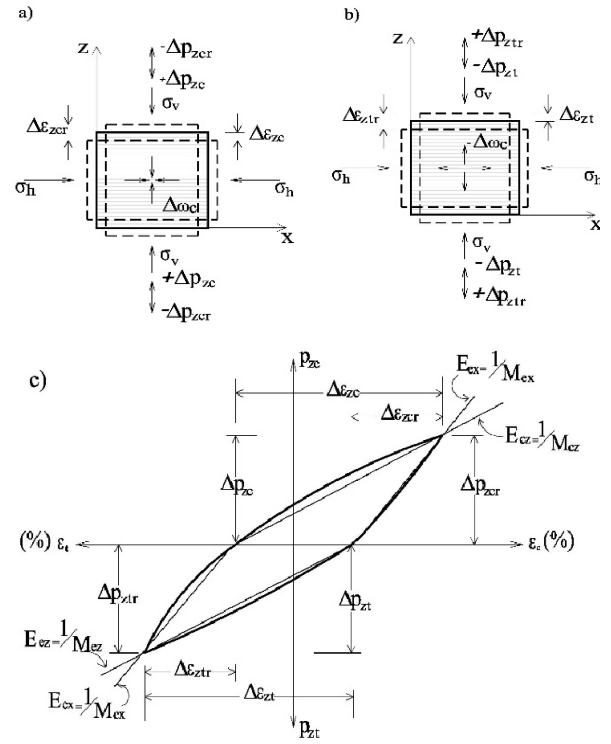


Figure 3. Definition of the parameters of the Zeevaert model for a stress-controlled cyclic triaxial test on a soil specimen. a) Stress state under compression; b) Stress state under tension; c) $(\pm \Delta p_z)$ - $(\pm \Delta \varepsilon_z)$.

CHARACTERISTICS OF THE TESTED SOIL, CYCLIC TRIAXIAL TESTS, AND RESULTS

3.1 Index and mechanical properties of the studied soil (clay from the Valley of Mexico).

The studied soil comes from the lacustrine zone of the Valley of Mexico, known as the Lake Zone, characterized by the presence of thick layers of highly compressible and low shear strength clay. Undisturbed samples were obtained with Shelby thin-walled tubes, 10 cm in diameter, at average depths of 4.0 and 6.5 m. It is a clay of very soft consistency (CH), showing some degree of preconsolidation in the field (OCR) less than 2, and dark gray color. The average index properties of saturated soft clays used in this investigation were: water content $w=200\%$; plastic index $PI=160\%$; specific gravity $G_s=2.3$; natural unit weight $\gamma_m = 13.0 \frac{kN}{m^3}$. The groundwater level was found at a depth of 5.5 m.

The samples index properties used in this investigation are reported in Table 1.

Table 1. Samples index properties

Sample	z (m)	W (%)	PI (%)	e_0	γ_m ($\frac{kN}{m^3}$)	OCR
M-09 (CH)	5.50	188.7	187.0	4.20	12.80	-
M-11(CH)	6.80	169.9	162.0	3.79	13.14	2.00

3.2 Cyclic triaxial and resonant column tests results

To obtain the dynamic parameters of the soft clays Mexico City (deformations moduli M_z , and material damping, λ) a series of cyclic triaxial tests were performed on natural specimens, under undrained conditions. The tests were in stress-controlled mode,

using frequencies of 0.5 and 1.0 Hz as this is a representative value for most earthquakes in Mexico City. The number of load cycles was $N = 20$, for each increment, until failure was reached. Once the clay specimens were consolidated to the equivalent effective in-situ stress state (σ'_{co}), they were subjected to a normal cyclic deviator stress. Increasing increments of cyclic deviator stress $\pm\Delta p_z$ were applied until the specimen failed.

To determine the values of the dynamic modulus of deformation at small strain levels, resonant column tests were conducted on soft clay specimens with similar characteristics to those used in cyclic triaxial tests, allowing for an adjustment of the experimental results.

Figure 4 shows the method for evaluating the deformation modulus M_z for a hysteresis cycle.

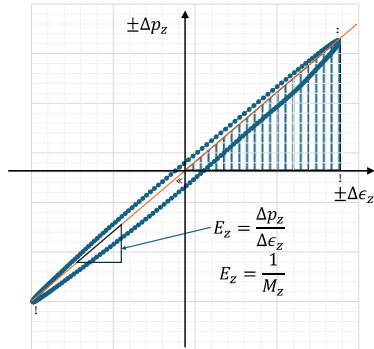


Figure 4. Determination of dynamic deformation moduli $M_z = 1/E_z$ and material damping λ .

3.2.1 Poro pressure

Figure 5 shows the pore pressure $2\Delta\omega$, as a function of linear strain, $2\Delta\varepsilon_z$, frequency 1.0 Hz, measured at the base and head of the specimens M09 and M11, for 50% of the failure deviatoric stress, $N = 10$ loading cycles, and consolidation stresses σ'_{co} of 132 and 220 kPa, respectively. This figure shows that the pore pressure at the base is higher than at the top, by approximately 14 kPa, for the peak of hysteresis loop, and for both confinement pressure. For the case of the specimen M-09, frequency 0.5 Hz, under consolidation pressure σ'_{co} of 100 kPa, the result is almost the same, the difference between base and head are 13 kPa. These results indicate that the linear strains caused by the application of cyclic deviatoric stress are not uniform throughout the soil specimen at least for the frequencies used in this investigation. Consequently, measuring these

deformations with the displacement transducer located outside the cyclic triaxial chamber does not accurately represent their true behavior. It is evident that the hysteresis loop obtained during the test are affected by this phenomenon, and therefore, the derived values of deformation moduli and material damping are also influenced.

3.2.2 Dynamic deformations modulus

Figure 6 shows the variation of the deformation modulus M_z as a function of the strain level $\Delta\varepsilon_z$, for the loading cycle $N=10$, cyclic frequency $f=1.0$ Hz, and for the samples M-9 and M-11, calculated from a cyclic triaxial test (Figure 3) under a confining stress of 0.135 and 0.220 MPa, respectively, combined with a resonant column test on a soil sample with similar characteristics under confining stresses of 0.039 , 0.118 , and 0.216 MPa. The experimental results were fitted using the behavioral model by (González and Romo, 2011) which is a function of the following parameters: minimum and maximum deformation moduli, M_{min} and M_{max} , respectively; the reference strain $\Delta\varepsilon_{rM}$, a value associated with the inflection point of the $M_{cz}-\Delta\varepsilon_{cz}$ curve; the strain level of the test $\Delta\varepsilon_{cz}$; and the experimental constant B_M , the latter being a function of the soil plasticity index PI . The values of the model parameters are reported in the same Figure 6.

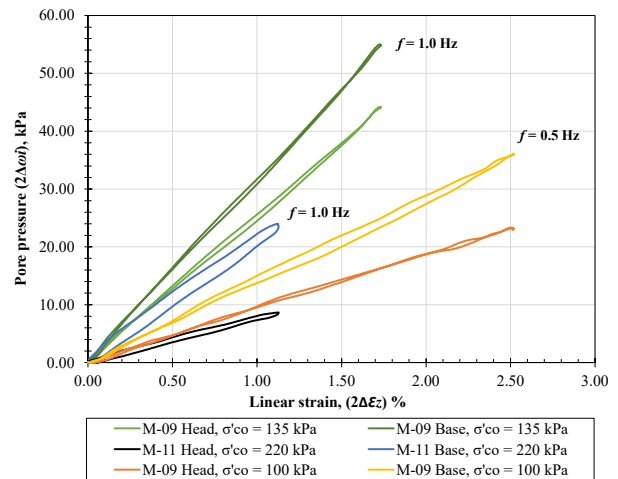


Figure 5. Pore pressure at the head and base specimen as a function of linear strain

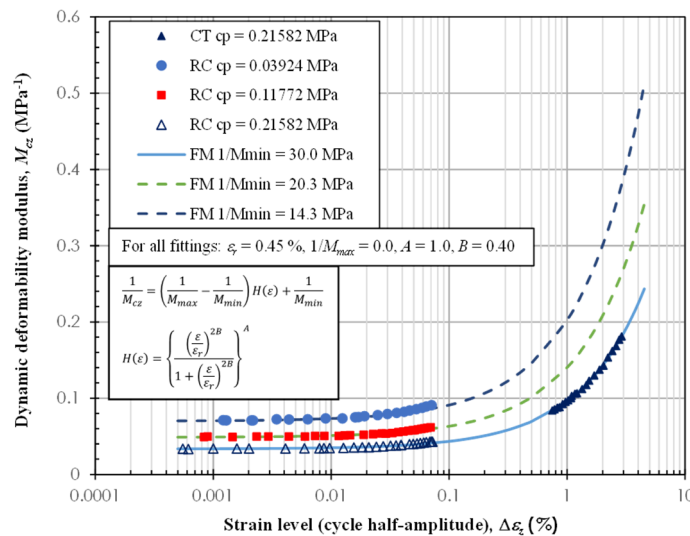


Figure 6. Deformation modulus M_z determined in the cyclic triaxial chamber (CT) and the resonant column (RC), as a function of the linear strain $\Delta\varepsilon_z$

3.2.3 Material damping

The material damping λ is associated with the energy dissipated as heat due to irreversible internal deformations that occur in the material during load-unload cycles. The energy dissipated in each load-unload cycle is related to the area of the hysteresis loop in the material's stress-strain curve. The material damping value can be calculated using the following equation:

$$\lambda = \frac{A_c}{4\pi A_t} \quad (15)$$

Where A_c is the area of the hysteresis loop and A_t is the area of the triangle OAB (Figure 4).

Figure 7 shows the variation of the material damping ratio λ as a function of the linear strain level $\Delta\varepsilon_z$ for samples M-9 and M-11, calculated from a cyclic triaxial test under a confining stress $\sigma'_{co} = 0.22$ MPa, combined with a resonant column test on a soil sample with similar characteristics under confining stresses of 0.04, 0.12, and 0.22 MPa. The same Figure 6 also displays the fitting of the experimental results using the Romo's model (González and Romo, 2011) which is a function of the following parameters: minimum and maximum material damping λ_{min} and λ_{max} , respectively; the reference strain $\Delta\varepsilon_{r,\lambda}$, a value associated with the inflection point of the $\lambda_{CZ} - \Delta\varepsilon_{CZ}$ curve; the strain level of the test $\Delta\varepsilon_{CZ}$; the experimental constant H_λ , which is in turn a function of a parameter defining the geometry of the $\lambda_{CZ} - \Delta\varepsilon_{CZ}$ curve, denoted as B_λ . The authors of the model have been able to express this last parameter as a function of the PI. The values of the model parameters are reported in the same Figure 7.

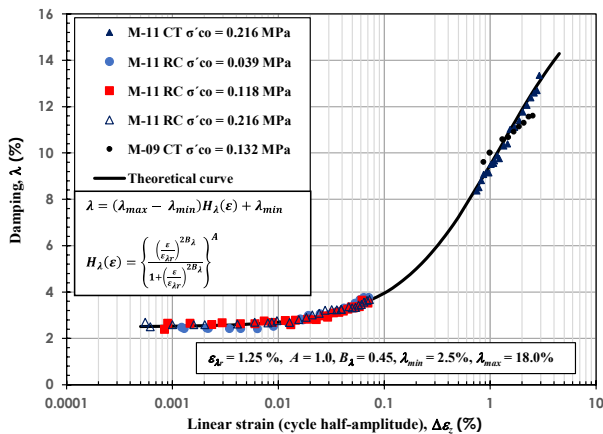


Figure 7. Material damping λ determined in the resonant column and in the cyclic triaxial chamber, as a function of linear strain $\Delta\varepsilon_z$

3.2.4 Poro pressures and dynamic deformations moduli. Zeevaert's model

Figure 8 shows the variation of the experimental and theoretical pore pressures $\pm\Delta\omega_i$ with the cyclic axial strain level $\pm\Delta\varepsilon_z$ for the sample M-11 ($\sigma'_{co} = 135$ kPa), computed for $\pm\Delta p_z / (\pm\Delta p_z)_f$ equal to 0.25, 0.50, 0.75 and 0.90, and for the loading cycle $N = 10$ and cyclic frequency 1.0 Hz. It is observed that the analytical pore pressures are higher than the measured ones at the base and the average base-head, but the maximum differences do not exceed 18 kPa. In the case of the cyclic test, sample M-11, $\sigma'_{co} = 216$ kPa (Figure 9), the measures pore pressure at the base were higher than the analytical values, but the maximum differences do not exceed 12 kPa. The average measures pore pressures are more similar

to the analytical values, with differences maximum and minimum of 10 kPa and 3 kPa, respectively.

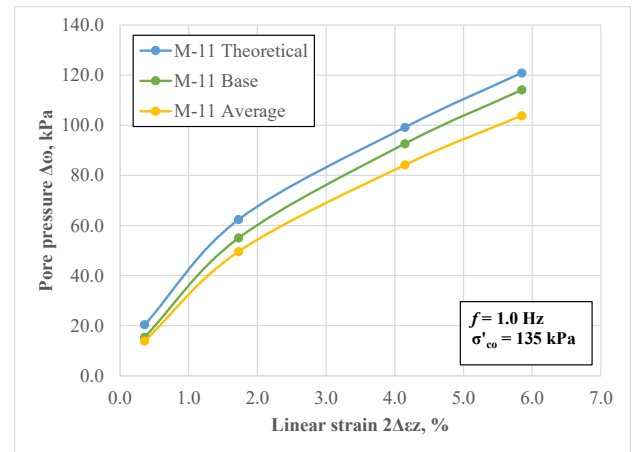


Figure 8. Experimental and calculated (Zeevaert model) pore pressures ($\pm\Delta\omega_i$) as a function of cyclic linear deformation level ($\pm\Delta\varepsilon_z$)

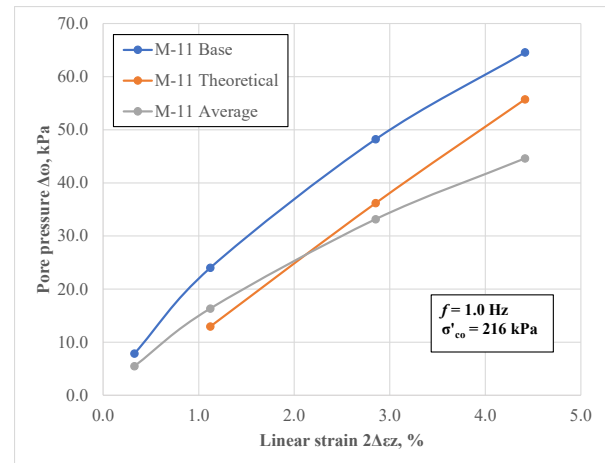


Figure 9. Experimental and calculated (Zeevaert model) pore pressures ($\pm\Delta\omega_i$) as a function of cyclic unit strain level ($\pm\Delta\varepsilon_z$)

All cyclic triaxial tests performed were interpreted from Zeevaert model (Zeevaert, 1988) thereby evaluating the corresponding parameters M_{cx} , M_{ex} , M_{cz} , and M_{ez} , using the equations (9), (10), (12) and (13), respectively.

Figure 10 shows the variation of the arithmetic average dynamic deformation moduli M_{cx} , M_{ex} , M_{cz} , and M_{ez} , as a function of the linear strain $\Delta\varepsilon_z$, for $\pm\Delta p_z / (\pm\Delta p_z)_f$ equal to 0.25, 0.50, 0.75 and 0.90, and load cycle $N = 10$. This figure also shows the dynamic deformation moduli but calculated as is indicated in Figure 4. It is observed that the dynamic deformations moduli calculated using de Zeevaert model for the specimen M-09, $\sigma'_{co} = 0.132$ MPa), are higher than that calculated from Figure 4, with differences maximum and minimum of 0.07 MPa^{-1} and 0.02 MPa^{-1} , respectively. It should be noted that in the case of the maximum difference, the theoretical module is 27% greater than the measured one. In the case of the cyclic test specimen M-11, $\sigma'_{co} = 0.216$ MPa, the theoretical and the experimental results are almost the same.

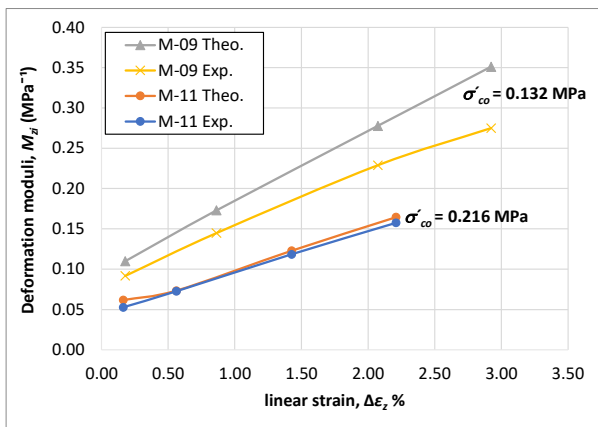


Figure 10. Variation of the arithmetic average dynamic deformation moduli M_{cx} , M_{ex} , M_{cz} , and M_{ez} with the cyclic axial strain level $\pm\Delta\epsilon_z$ compared with experimental moduli (Fig. 3)

4 CONCLUSIONS

A series of cyclic triaxial tests were conducted on soft clays from Mexico City (CDMX), measuring the pore pressures generated during the application of deviatoric stress at the top and base of the specimens. Although the observed maximum differences for pore pressure are relatively small, and do not exceed 18 kPa, in all the tests, this revealed the non-uniformity of deformations induced during cyclic deviatoric stress application which affect the values of dynamic deformation moduli. These moduli were calculated using both the traditional method (ignoring pore pressures) and the Zeevaert model (analytically estimated pore pressures). It was found that the dynamic deformations moduli calculated using de Zeevaert model for the specimen M-09, $\sigma'_{co} = 0.132$ MPa), are higher than that calculated from Figure 3, with maximum and minimum differences, of 0.07 MPa $^{-1}$ and 0.02 MPa $^{-1}$, respectively. In the case of the cyclic test specimen M-11, $\sigma'_{co} = 0.216$ MPa, the theoretical and the experimental results are the same. Apparently, the confinement pressure has some influence on the differences found between the measurement and theoretical values for the dynamic deformation moduli, which should be clarified in future investigations.

Regarding material damping, there is no theoretical framework available to date to correct the hysteresis cycle due to the pore pressures generated during the application of the cyclic deviator stress.

It is worth noting that the measures pore pressure at the base of the specimens were higher than that at the head, indicated that the linear strains caused by the application of cyclic deviatoric stress are not uniform throughout the soil specimen at least for the frequencies used in this investigation (0.5 and 1.0 Hz). These results justify the need, in future research, to determine the true pore pressure distribution within the specimen. To achieve this, a miniature pore pressure transducer should be installed at the mid-height of the specimen (on the periphery), at the same time it is also important to investigate the effect of the confinement pressure magnitude and frequency of application of the deviator stress on the pore pressure distribution along the specimen.

5 ACKNOWLEDGEMENTS

The authors of this work would like to express their deepest gratitude to the Dirección General de Asuntos del Personal Académico (DGAPA) of UNAM for the financial support provided through the Programa de Apoyo a Proyectos de Investigación y Desarrollo Tecnológico (PAPIIT), project IG100324.

Likewise, we wish to extend our appreciation to the authorities of the División de Ingenierías Civil y Geomática (DICyG) and the Instituto de Ingeniería (II) for allowing us to participate in this multidisciplinary project, the final outcome of which was the development of this publication.

We cannot overlook the unconditional support provided by the staff of the Geotechnics Laboratory of DICyG and II, both during the setup of the automated cyclic triaxial equipment and throughout the experimental stage.

6 REFERENCES

- Gasparre, A., Nishimura, S., Minh, N.A., Coop, M.R. and Jardine, R.J., 2007. The stiffness of natural London Clay. In: *Geotechnique*. <https://doi.org/10.1680/geot.2007.57.1.33>.
- González, C. and Romo, M., 2011. Estimación de propiedades dinámicas de arcillas. *Revista de Ingeniería Sísmica*, 84(123).
- Huang, J., Hu, J., Wang, H., Chen, J. and Liu, S., 2023. Excess pore water pressure behavior of saturated soft clay under cyclic confining pressure with different frequencies. *Frontiers in Earth Science*, 10. <https://doi.org/10.3389/feart.2022.1035889>.
- Hyodo, M., Yamamoto, Y. and Sugiyama, M., 1994. Undrained cyclic shear behaviour of normally consolidated clay subjected to initial static shear stress. *Soils and Foundations*, 34(4). https://doi.org/10.3208/sandf1972.34.4_1.
- Josseume H., 1971. Etude de la presión interstitielle, Raport de Recherche (14). *Laboratoire de Ponts et Chaussées*, Ministère de l'équipement et du logement. France.
- Kimura, T. and Saitoh, K., 1983. Influence of strain rate on pore pressure in consolidated undrained triaxial tests on cohesive soils. *Soils and Foundations*, 23(1). <https://doi.org/10.3208/sandf1972.23.80>.
- Mendoza, M. and Hernández, V., 1994. Pore-pressure build-up under cyclic loading in México City clay. In: *XIII International Conference for Soil Mechanics and Geotechnical Engineering*. New Delhi, Ende. pp.181–186.
- Ovando, E., Hernández, Z., Flores, O. and Fernández, A., 2021. Cyclic behaviour and dynamic properties of Texcoco clays near México City. *Geotechnical Engineering Journal of SEAGS & AGSSEA*, 52(4), pp.33–38.
- Rivera, R., Zea, C., Flores, O., Gómez, E., Ossa, A., Arias, R. and Elizalde, E., 2024. Determinación de los módulos de deformación unitaria dinámicos usando un equipo triaxial cíclico automatizado. Modelo de Zeevaert. In: *17th Panamerican Conference on Soil Mechanics and Geotechnical Engineering*. La Serena, Chile.
- Rojas, E., Romo, M.P. and Hiriart, G., 1990. Estudio de la presión de poro al centro de probetas. In: *15 Reunión Nacional de Mecánica de Suelos*. San Luis Potosi, México: Sociedad Mexicana de Ingeniería Geotécnica. pp.111–118.
- Soralump, S. and Prasomsri, J., 2016. Cyclic Pore Water Pressure Generation and Stiffness Degradation in Compacted Clays. *Journal of Geotechnical and Geoenvironmental Engineering*, 142(1). [https://doi.org/10.1061/\(asce\)gt.1943-5606.0001364](https://doi.org/10.1061/(asce)gt.1943-5606.0001364).
- Yasuhara, K., Yamanouchi, T. and Hirao, K., 1982. Cyclic Strength and Deformation of Normally Consolidated Clay. *Soils and Foundations*, V22(N3), pp.77–91. https://doi.org/10.3208/sandf1972.22.3_77.
- Zeevaert, L., 1988. *Sismo-geodinámica de la superficie del suelo*. 1a ed. CDMX, México.